Extended Abstracts of the 16th (1984 International) Conference on Solid State Devices and Materials, Kobe, 1984, pp. 441-446

Invited

Photo-Excited Dry Etching for VLSI's

Y. Horiike, M. Sekine, K. Horioka, T. Arikado and H. Okano

Toshiba VLSI Research Center, Toshiba Corporation
1, Toshiba-cho, Saiwai-ku, Kawasaki, 210 Japan

UV light-excited etching of various types of poly-Si and single-Si in $C\ell_2$ has been studied. Undoped poly-Si etching proceeds toward a photo-irradiation direction. The result was applied successfully to the resistless etching which was performed by IC pattern transfer to the sample. On the other hand, n^+ poly-Si is etched isotropically. The anisotropic n^+ poly-Si etching was also achieved by forming the passivation film on the etched sidewall with photo-excited deposition. When O_2 is added to $C\ell_2$ of a Si etching gas, a new selective Si oxidation has been developed. This is an atractive technique for field isolation, while problems for the film structure still remain.

1. Introduction

Reactive Ion Etching (RIE) has contributed greatly to the recent rapid progress on VLSI devices. However, energetic charged particles of ions and electrons in the plasma cause various radiation damages to devices. Especially, the gate-oxide-breakdown phenomena after the gate material RIE(1) imply that prospects are gloomy for achieving finer dimension devices. Thus, photo-excited processes(2,3), which do not use charged particles, are noted aiming at no radiation damage. These studies in turn are useful for understanding detailed kinetics of RIE.

This paper reports UV light-excited etching characteristics of silicon, and their applications to the undoped poly-Si resistless etching and the n^+ poly-Si anisotropic etching. Finally, selective Si oxidation is presented briefly.

2. Experimental

Figure 1 shows a schematic illustration of the etching system. At first, a high-pressure Hg-Xe lamp was used as a light source(4), and then it was changed by the present excimer laser(5). The excimer laser operated on 308 nm $XeC\ell$ line at pulse width of 80 pps emits 10x20 mm^2 sheet beam, which is irradiated through a quartz lens to a sample surface. The sample is set in a reaction chamber filled with 10~100 torr $C\ell_2$. The average power was about $3W/cm^2$ on a sample surface. In

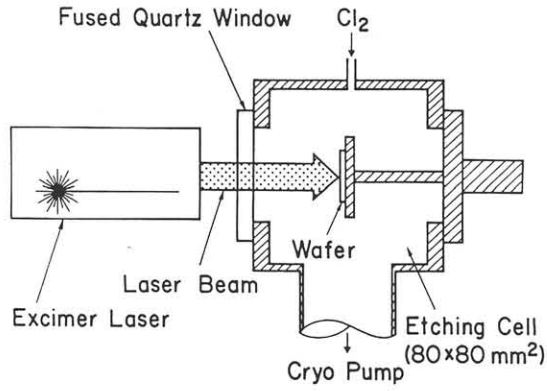

Fig. 1 Excimer laser etching system.

the case of the Hg-Xe lamp, it was focused to 2 mm ϕ dia. (275 mW/cm^2) on the surface. Both Hg-Xe lamp and $XeC\ell$ laser can dissociate directly an excited $C\ell_2$ gas with a 300~400 nm absorption peak to produce $C\ell$ atoms. Both sources provide same order poly-Si etch rates.

Samples to be etched were phosphorus(P) or boron (B) ion implanted to the undoped poly-Si and the single-Si. The $A\ell$ and SiO_2 films were used as etching masks, respectively. A sample was mounted on the sample holder after dipping in the BHF solution to remove the native oxide. Etching experiments were carried out by a mechanical pump after evacuation to a pressure below 10^{-6} torr.

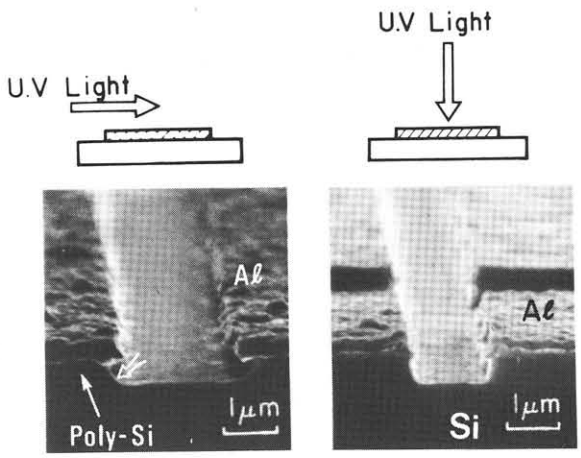

(a) (b)

Fig. 2 Etched feature of P doped, (a) and undoped poly-Si, (b). The arrow in (a) shows the undercutting.

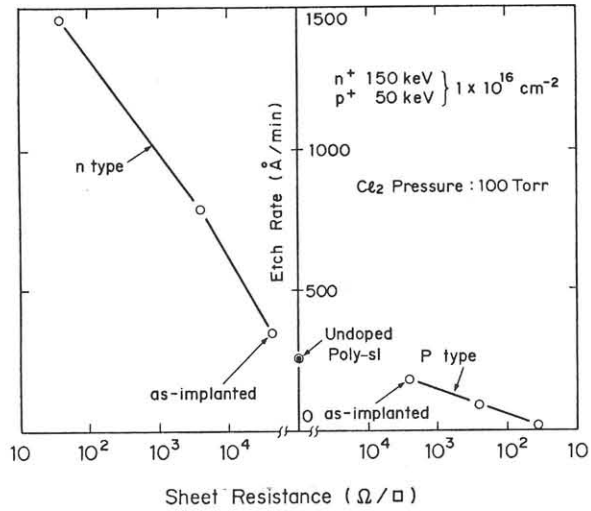

Fig. 3 n, undoped and p type poly-Si etch rates vs. sheet resistance.

3. Etching Results and Reaction Mechanism

Results shown in figures of 2 and 3 were obtained using the Hg-Xe lamp. Figure 2 shows SEM cross-sectional micrographs of etched features of the P doped, (a) and the undoped poly-Si, (b). The n^+ type poly-Si is etched isotropically by Cℓ radicals generated by the UV irradiation to the gas phase as well as on the surface. On the other hand, both undoped and p type poly-Si etchings proceed toward a photo-irradiation direction to demonstrate an anisotropic feature. This result is analogous to the ion-assisted chemical etching in the RIE process.

Figure 3 shows variations of n, undoped and p type poly-Si etch rates as a function of sheet resistance, where the abscissa sales in n and p type are expressed inversely. P and B ions were implanted at 150 and 50 keV accelerating voltage under the same $1x10^{16}cm^{-2}$ dosages. The sheet resistance was changed by 40 min, 550°C and 10 min, 1000°C heat treatments, respectively, where dopant concentrations were assumed to be uniformly distributed within films. The etch rates decrease in order of n^+,n, undoped, p and p^+ types. The etchings of undoped and p types occur when the surface is irradiated with photons, in other words, when hole-electron pairs are generated. Considering that electrons are a minority carrier in the p-type Si, therefore this etch rate order corresponds quite to electron concentrations in conduction band, as indicated in the abscissa.

The faster etch rate of the n^+ type Si is well-known in the halogen atom containing plasma. Based on this plasma etching mechanism[6,7], the photo-excited reaction is assumed as follows[3]. At first, photo-dissociated Cℓ atoms adsorb on the Si surface. Simultaneously, the separation of photo-electron and hole pairs and their different carrier mobilities produce the surface electric field[8]. Eventually, it can cause a band bending [9] and facilitate the charge transfer from silicon to the adsorbate Cℓ species. The negatively charged species, $C\ell^-$ can penetrate into Si lattices and then, reaction products of $SiC\ell_x$ (x=1~4) are desorbed to the gas phase. Hence, n^+ type Si with about 10^{21} cm^{-3} electrons is etched spontaneously by sufficient $C\ell^-$ ions. However, at present, no actual effect such as etch rate dependences on the electric field has been verified. Besides, the high energy UV light is considered to break the material bondings. The more intensive studies are required for the photo-excited reaction.

4. Resistless Etching[4,5]

It can readily be assumed that this anisotropic feature obtained for the undoped poly-Si is applicable to the resistless etching. As shown in Fig. 4(a), the opaque Aℓ film mask pattern prepared on a quartz plate is set in close proximity to the sample surface in the $C\ell_2$ gas. Figure 4(b) shows that a fine etching pattern less than 1 μm.

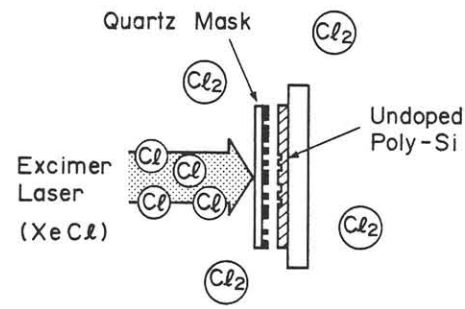

(a)

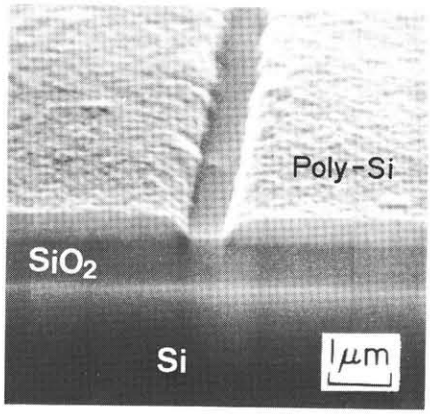

(b)

Fig. 4 Resistless etching. (a): Etching method, (b): a example of a fine pattern.

More exact and finely etched features will be attainable by employing a short-wavelength optical projection system. This resistless etching enables us to cut the present lightography processes and hereby will offer a great improvement over the future VLSI processings.

5. n^+-Type Poly-Si Anisotropic Etching[10]

The n^+ poly-Si anisotropic feature achieved by RIE results from the passivating film formation on the etched sidewalls, which protects undercuttings caused by the radical attack[10]. The photo-excited process also allows this anisotropic n^+ poly-Si etching using an analogous mechanism to RIE.

Figure 5 illustrates schematically the present photo-excited etching concept. A Hg-Xe lamp, which irradiates parallel to a n^+ poly-Si surface dissociates $Si(CH_3)_4$ in the presence of Hg sensitizers to produce an a-SiC like film on the surface. At the same time, XeCℓ excimer laser is incident normally to the wafer in $C\ell_2$. Accordingly, it can be assumed that only laser-irradiation surface is etched and simultaneously, the film

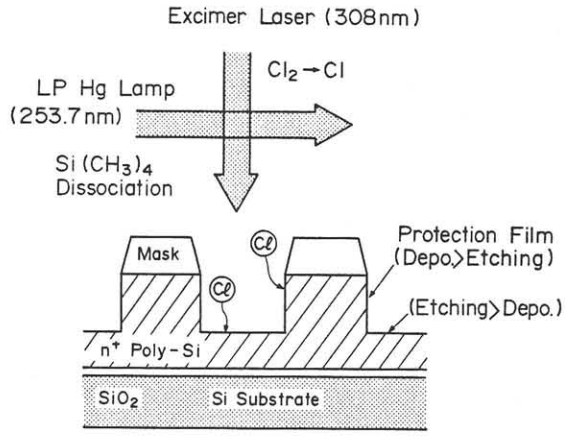

Fig. 5 Conceptual illustration of the n^+ poly-Si anisotropic etching method.

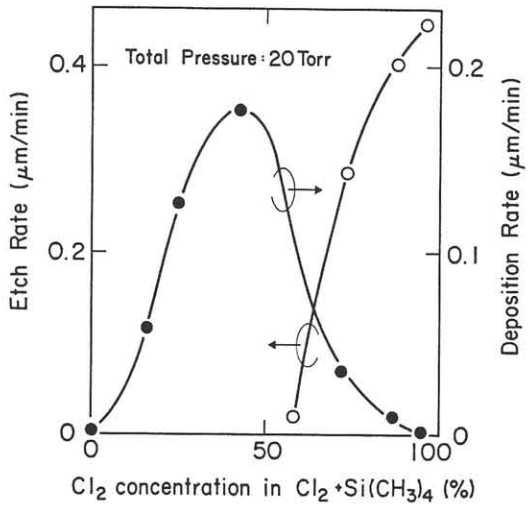

Fig. 6 n^+ poly-Si etch rate and film deposition rate vs. % $C\ell_2$ in Si $(CH_3)_4$.

deposition occurs only on the sidewall.

Figure 6 shows variations of n^+ poly-Si etch rates and film deposition rates as a function of % $C\ell_2$ in a $C\ell_2$ + $Si(CH_3)_4$ mixture. Total pressure is kept at 20 torr. The deposition rate was measured from a deposited film on the SiO_2 substrate, since SiO_2 is not etched at all. In the absence of $C\ell_2$, the deposition rate is unexpectedly low even in the Hg sensitization condition. However, the deposition rate increases rapidly with $C\ell_2$ addition. This result suggests that Cℓ radicals dissociate $Si(CH_3)_4$ as a result of their collision in the gas phase and also react with $Si(CH_3)_4$ to generate nonvolatile products. Indeed, an IR measurement shows appreciable C-Cℓ bond in this film. This film can be easily removed by an organic solvent. For subsequent $C\ell_2$ addition, the

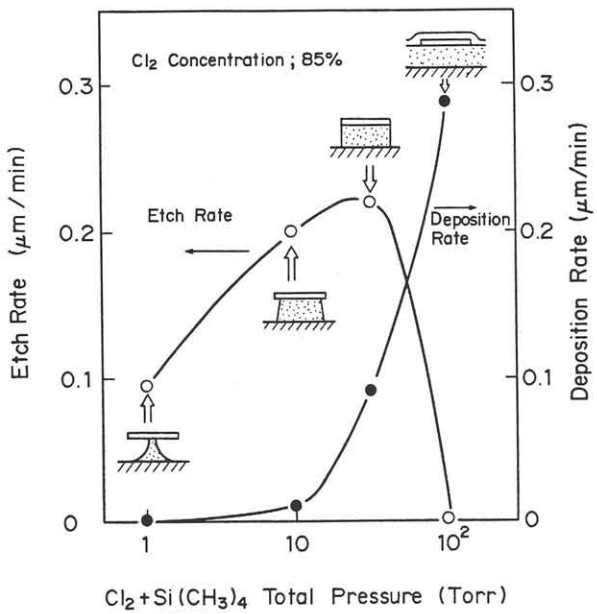

Fig. 7 n^+ poly-Si etch rate and film deposition rate vs. $C\ell_2$+Si$(CH_3)_4$ total pressure under 85% $C\ell_2$ concentration. Corresponding etched feature are also inset.

n^+ poly-Si etch rate begins to increase more than 50% $C\ell_2$ concentration to contrast with decrease in the deposition rate, and then exceeds the deposition rate for more $C\ell_2$ addition.

As shown in Fig. 7, under the condition of 85% $C\ell_2$ concentration, both etch and deposition rates were measured as a function of total pressure. The related etching morphologies are also inset in this figure. The lower pressure around 1 torr provides the etching alone, thus an isotropic feature is observed. However, the undercutting is reduced with increase in pressure, which enhances both etch and deposition rates. Eventually, an anisotropic feature can be attained around 30 torr, where the etch rate attains a maximum and the deposition takes place abruptly. Thereafter, etch rates fall down and the film covers completely on the patterned surface, at 100 torr. It can be concluded that the photo-excited technology performes the similar RIE process. As shown in Fig. 8, the anisotropic feature has been successfully obtained.

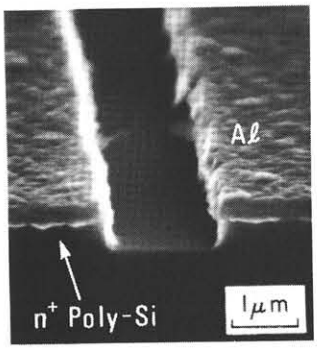

Fig. 8 Anisotropic etched feature of n^+ poly-Si. Etching pressure is 30 torr.

Electrical influences have been also investigated using MOS capacitors with 50 Å gate oxide, which are fabricated by RIE and the laser etching. The serious gate oxide breakdown by RIE occurred, while the present XeCℓ case demonstrated same good tolerance as a wet chemical reference. Thus, the photo-excited etching is considered to become a powerful technology for submicron MOS devices, because the very thin underlying oxide is never etched by this method. However, the higher energy laser irradiation such as ArF (193 nm) should be investigated on the radiation damages.

6. Single-Si Etching(5)

Corresponding to Fig. 3, single-Si etching characteristics were also studied. Figure 9 shows variations of etch rates of n type and p type single-Si as a function of sheet resistance with crystallographic orientations of (100) and (111) as a parameter. The p type Si is not etched without photoirradiation. Therefore, based on the earlier discussion in 3., the abscissa is scaled in the direction of decrease in the amount of electrons in the conduction band. Since etch rate differences between both planes in heavily doped n type are small, an etched feature shows a quasi-isotropic profile. However, with decrease in the amount of electrons in the conduction band, etch rates of both types and planes decrease and especially, the (111) etch rate is reduced rapidly.

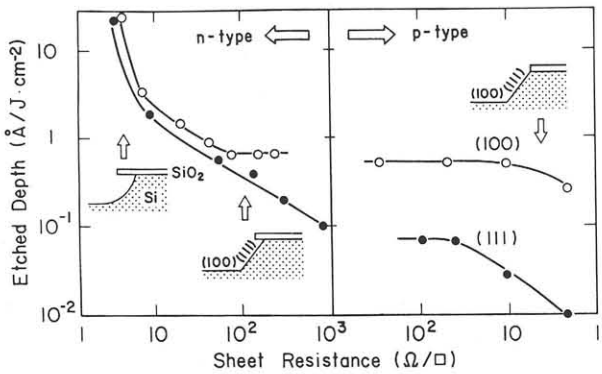

Fig. 9 Etch rate of n and p type single-Si vs. sheet resistance with crystallogrphic orientation of (100) and (111) as a parameter. Corresponding etched features are also inset.

Thus, the preferential sidewall orientation (111) can be observed for the (100) plane. The origin of the low etch rate in the p type Si is supposed that $C\ell^-$ ion penetration into Si is not easier in the closed-packed(111) plane than that in the (100) plane. The anisotropic feature leads to the next application.

7. Selective Single-Si Oxidation[12]

A new photo-excited single-Si oxidation has been found when O_2 gas is added to $C\ell_2$ gas. As shown in Fig. 10, the Si surface, which is not masked by thermally-grown SiO_2, is easily oxidized with a $C\ell_2 + O_2$ mixture at 250°C. The AES and IR measurements of this film indicate a stoichiometric Si oxide structure. Parallel as well as normal laser (308 nm) irradiations to the Si surface produce this oxidation, while the rate in the parallel case is about 1/5 times of the normal case. It should be noted that the oxidation does not take place, unless the native oxide is etched with BHF dipping.

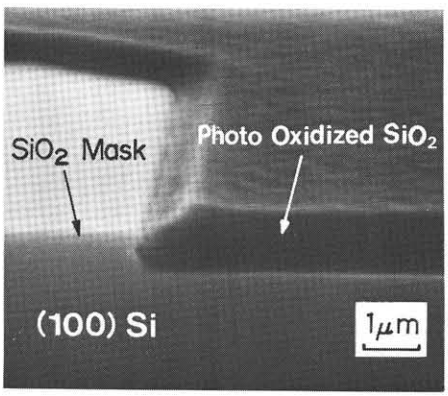

Fig. 10 Cross-sectional view of the selective oxidized feature.

Figure 11 shows variations of Si etched depths and oxidized layer thicknesses as a function of O_2 pressure at 250°C. Oxidation time is fixed at 10 min. Very high etch rate of 1700 Å/min is observed employing $C\ell_2$ alone. The Si etch rates decrease with increasing O_2 pressure, because of recombination of photo-dissociated $C\ell$ atoms due to the shorter mean free path. On the other hand, the oxidation grows rapidly. In this region, the oxidation seems to be produced by supplying O_2 gas to the sufficient Si etching products. After a maximum oxidation rate at 100 torr O_2 pressure, the oxidation rates decrease

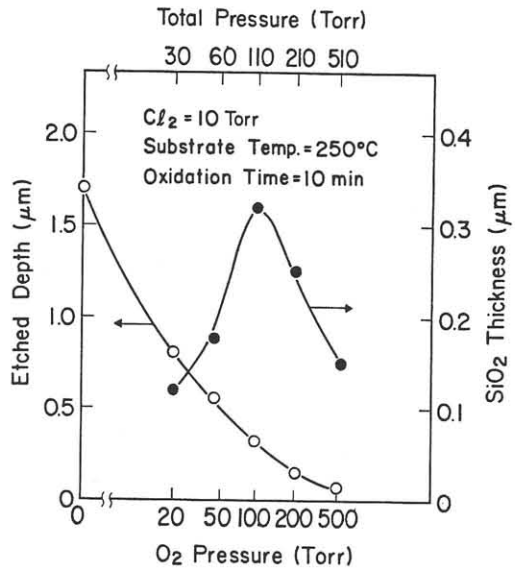

Fig. 11 Si etched depth and oxide layer thickness vs. O_2 pressure at a fixed $C\ell_2$ pressure.

with increasing O_2 pressure. This oxidation process is limited by the scarce Si source. Accordingly, the following reaction process is proposed.

$$C\ell_2 \xrightarrow{h\nu} 2C\ell$$

$$Si + xC\ell \rightarrow SiC\ell_x$$

$$SiC\ell_x + O_2 \rightarrow SiO_2 + \frac{x}{2} C\ell_2$$

, where $SiC\ell_x$ is unsaturated Si chlorides with x=1~3. As a preliminary experiment, the photo-oxidation was tried employing $SiC\ell_4 + O_2 + C\ell_2$. But only 5 Å/min oxidation rate was obtained. Thus, the $SiC\ell_x$ is assumed to have more active chemical reactivity than the stable $SiC\ell_4$.

Since the oxide surface level can be changed for the Si surface level, the new process may be used for the planarized field isolation. However, the BHF etch rate shows very high value of 0.4 μm/min even at 800°C annealing in O_2 ambience. The film structure should be improved.

8. Conclusion

Taking consideration into the radiation damage caused by plasmas, a photo-excited process has been studied. As a result, similar fine line poly-Si engraving to RIE was achieved, in spite of the small-scaled and insufficient feature. Also, the resistless etching possibility was found.

However, a lot of problems have to be solved for further development: namely, Aℓ and SiO_2 anisotropic etching, rate limiting process for high reactivity, from gas phase to surface reaction, the high rate pulse and large area excimer laser and a short-wavelength optical system, etc. Especially, intensive studies are required for the fundamental reaction process on the surface.

Reference

1. T. Watanabe and Y. Yoshida, Sol. St. Technol.,/ April (1984) 263.
2. D.J. Ehrlich and J.Y. Tsao, "VLSI Electronics: Microstructure Science Vol. 7" eds. N. Einspruch (Academic, N.Y. 1983) 129.
3. T.J. Chuang, Surf. Sci. Reps. 3(1981) 1.
4. H. Okano, Y. Horiike and M. Sekine, Electrochem. Soc. Spring Meeting, Ext. Abs. No.430(1983).
5. T. Arikado, M. Sekine, H. Okano and Y. Horiike, Mat. Res. Soc. Fall Meeting Abs. I9.5 (1983) 408
6. D.L. Flamm and V.M. Donnelly, Plasma Chem. Plasma Process, 1 (1981) 330.
7. H.F. Winters, J.W. Coburn and T.J. Chuang, J. Vac, Sci. Technol., B1 (1983) 469.
8. R. Gauthier and C. Guittard, Phys. Status Solidi(a) 38 (1976) 477.
9. T.T. Tsong, Surf. Sci. 81 (1979)28.
10. H. Okano, Y. Sekine and Y. Horiike, to be published.
11. R.H. Bruce and G.P. Malafsky, Electrochem. Soc. Spring Meeting, Ext. Abs. No. 158 (1981).
12. K. Horioka, H. Okano and Y. Horiike, to be published.